ISSN 2354-0575

EFFECTS OF INDENTER RADIUS ON MECHANICAL PROPERTIES AND DEFORMATION BEHAVIOR OF $Cu_{50}Zr_{50}$ METALLIC GLASSES IN INDENTATION AND SCRATCHING PROCESS

Anh-Son Tran[1], Phan Thi Ha Linh[1, 2*]
1 Hung Yen University of Technology and Education
2 Hanoi University of Science and Technology
** Email: halinhcokhi@gmail.com*

Received: 02/08/2019
Revised: 22/08/2019
Accepted for publication: 10/09/2019

Abstract:

In this paper, a combination between the indentation and scratching process was developed to analyze the deformation mechanisms and mechanical properties of $Cu_{50}Zr_{50}$ metallic glasses (MGs) using molecular dynamics (MD) simulation. The deformation mechanisms and mechanical properties of $Cu_{50}Zr_{50}$ MGs are appraised through the surface morphology, pile-up height, hardness, machining forces, and resistance coefficient. The influences of different indenter radius are clearly investigated. The results exhibit that the machining zone increases as increasing indenter radius. The pile-up height and hardness reduce with a bigger radius of the indenter. The hardness values range from 7.94 to 13.33 GPa. The forces increase, however, the resistance coefficient decreases as the indenter radius increases.

Keywords: *$Cu_{50}Zr_{50}$ MGs; indentation; scratching; resistance coefficient.*

1. Introduction

Mechanical properties and deformation mechanisms are very typical and exceedingly important factors used to evaluate the characteristics of the materials. These factors directly influence the workability of the materials. Therefore, the investigation and evaluation on the mechanistic characteristics of materials are very necessary. Many experimental studies have been conducted to investigate the mechanical properties and the deformation mechanism of materials with different testing methods [1,2]. However, the sizes of the samples in the experimental studies are still quite large, in the microscale or macroscale. In order to assess the properties of materials more deeply and more accurately, the size of the material has been reduced to nanoscale. The nanoscale is a major barrier for the performing of experimental studies, requiring an alternative method. With the strong development of computer technology, molecular dynamics (MD) simulation method is an appropriate choice in simulating and evaluating the properties of nanomaterials. MD simulation method is simple and accurate in conducting the simulations with the testing processes are diverse such as shear, compression, indentation, tension, scratching, cutting, and so on.

In the modern industrial age today, MGs are widely used [3]. One of the most popular MGs systems is copper MGs type. Many systems of copper MGs have been created to study the structural, dynamic properties such as Cu-Mg [4], Cu-Zr [5], Cu-Ta [6], Cu-Ni [7]. Among these copper MGs systems, Cu–Zr MGs has emerged as the promising immiscible alloy systems for applications in electrical engineering, magnetic-sensing, chemical, and structural materials. The indentation and scratching processes are usually performed to study the mechanical properties and deformation mechanisms of materials, however, the combination of these two processes is scarce, especially with Cu-Zr MGs.

In this work, the mechanical properties and deformation mechanisms of $Cu_{50}Zr_{50}$ MGs systems are analyzed and evaluated through the combination of indentation and scratching processes using MD simulation. The machining processes are simulated with different indenter radius. The results will supply a more penetrating understanding of the mechanistic abilities of $Cu_{50}Zr_{50}$ MGs.

2. Methodology

The structure of a $Cu_{50}Zr_{50}$ MGs model at room temperature is created from the simulation

of melting and quenching process. The isobaric-isothermal ensemble (NPT) is used, the periodic boundary conditions (PBCs) are determined in three dimensions, and the pressure is conserved at zero during the simulation process. Firstly, the model is heated up to 2128 K (melting point of Zr component) at a heating rate of 2 K/ps. Then, the thermal equilibration process is kept at 2128 K for 500 ps. Finally, the model is cooled down to 300 K at a high cooling rate of 5 K/ps and then equilibrated at 300 K for 500 ps.

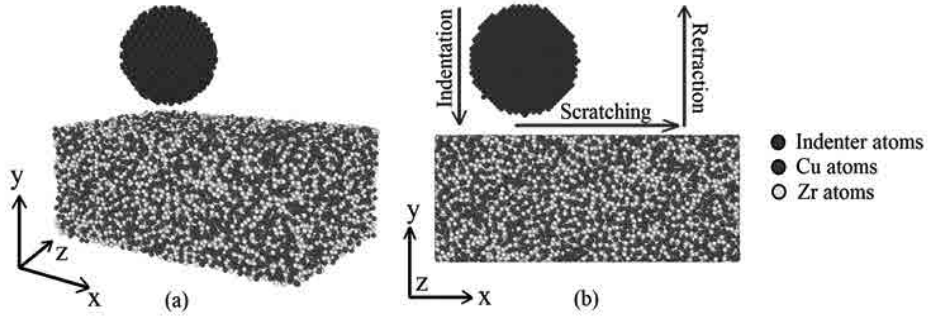

Figure 1. *The $Cu_{50}Zr_{50}$ MGs model for the indentation, scratching, and retraction system*

Figure 1 shows the $Cu_{50}Zr_{50}$ MGs model for the machining process. The machining system consists of a sphere diamond indenter and a $Cu_{50}Zr_{50}$ MGs specimen. The machining process is divided into three stages including indentation, scratching, and retraction. The indenter is considered an ideal rigid body to simplify the machining problem and focus on the deformation of the $Cu_{50}Zr_{50}$ MGs specimen. The different indenter radius are 1.5, 2.0, 2.5, and 3.0 nm. The dimensions of $Cu_{50}Zr_{50}$ MGs specimen are 15 nm (length) × 6 nm (height) × 10 nm (width) corresponding to x-, y-, and z-axis, respectively. Three types of atoms are set in the specimen, namely Newtonian atoms, thermostat atoms, and fixed atoms. The fixed atoms are made up of the four atoms layers. The substrate is fixed in the box by fixing three layers of substrate atoms at the bottom and next to the box margins in x- and z-axis to support the whole physical system during the machining process. The thermostat atoms are also constituted of the four atoms layers and placed between the fixed atoms and Newtonian atoms, which are used to maintain them at a constant temperature of 300 K by rescaling the velocities of these atoms every twenty-time steps. PBCs are determined in the x-, and z-axis, while the free boundary is applied along y-axis. The NVT (canonical ensemble) is used in the simulation. The initial distance between the indenter and the surface of the specimen is 1 nm. The machining process begins by the indentation stage with a machining depth of 2 nm and the indentation velocity of 50 m/s along y-axis. Then, the scratching stage is performed with a scratch distance of 5 nm and a scratch velocity of 50 m/s along the x-axis. Finally, the indenter retracts to the original position at a retraction velocity of 100 m/s.

The EAM potential proposed by Mendelev et al. [8] is employed to depict the interaction between Cu and Zr atoms. The atoms interaction between the indenter and $Cu_{50}Zr_{50}$ MGs is employed by the Lennard-Jones (LJ) potential [4]. The indenter is set as a rigid body, therefore the interaction between C atoms of the indenter is ignored.

Hardness is a very important factor to evaluate the mechanical properties of materials. The hardness value (H) is determined as

$$H = \frac{F_{max}}{A_c} \quad (1)$$

where F_{max} is the maximum normal force, Ac is the contact area between the indenter and specimen in the indentation stage. Ac is calculated as

$$A_c = \pi R h_c \quad (2)$$

where h_c is the indentation depth. The resistance coefficient (μ) is determined as follows:

$$\mu = \frac{F_t}{F_n} \quad (3)$$

where F_t and F_n is the tangential and normal forces in the scratching stage, respectively.

The Large-scale Atomic/Molecular Massively Parallel Simulator (LAMMPS) is employed to conduct all MD simulations. The Open Visualization Tool (OVITO) is used to present the processing data acquired from MD simulations.

3. Results and discussion

3.1. Dynamic response of $Cu_{50}Zr_{50}$ MGs

Figure 2(a) shows the lateral cross-sectional view of the pile-up and groove formed after the retraction of the indenter for the different indenter radius. The shear strain focuses more intensely in the case of smaller indenter radius. This indicates that the plastic deformation is more severe with a smaller indenter radius. Machining zone and pile-up height significantly decrease as the increasing indenter radius. Corresponding, the chipping volume is also clearly larger and more chippings are generated around the groove, which can be seen in Figure 2(b). It means that increasing indenter radius clearly affects the indentation and scratching characteristics of $Cu_{50}Zr_{50}$ MGs. As the indenter radius is relatively bigger, the contact area between indenter and substrate is larger leads to groove zone is larger. The materials around the indenter are concentrated and then obviously emerge on the surface with a smaller indenter radius, which are spread around the machining zone with a bigger indenter radius. So, the pile-up height on the surface is lower with a bigger radius of indenter in the machining process.

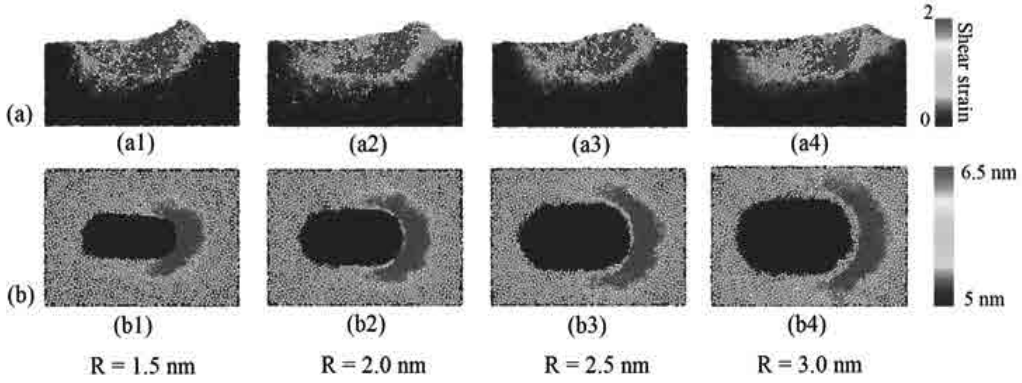

Figure 2. *(a) The lateral cross-sectional-view of the pile-up and groove formed after the retraction of the indenter and (b) the surface morphology of $Cu_{50}Zr_{50}$ MGs for the different indenter radius.*

A comparison between maximum pile-up height values of $Cu_{50}Zr_{50}$ MGs during indentation and scratching process with different indenter radius is shown in Figure 3. The maximum pile-up height values are 16, 13, 12, and 10 Å corresponding to indenter radius of 1.5, 2.0, 2.5, and 3.0 nm, respectively.

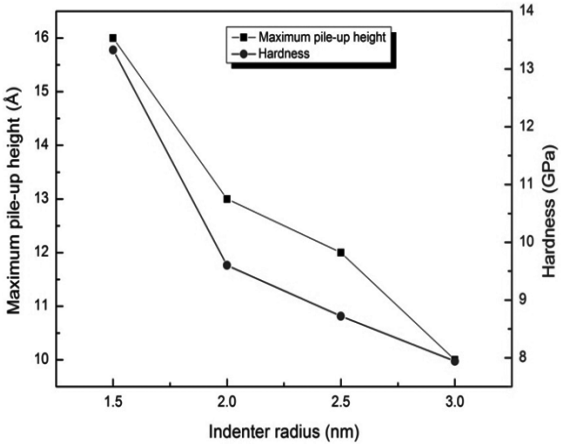

Figure 3. *The maximum pile-up height and the hardness of $Cu_{50}Zr_{50}$ MGs with different indenter radius*

Hardness is a typical factor to evaluate the mechanical properties of materials. The hardness values of $Cu_{50}Zr_{50}$ MGs at different indenter radius under the indentation process are also presented in Figure 3. The hardness values are 7.94, 8.72, 9.60, and 13.33 GPa corresponding to indenter radius of 1.5, 2.0, 2.5, and 3.0 nm, respectively. So, the hardness of $Cu_{50}Zr_{50}$ MGs reduces with the increasing indenter radius [9].

3.2. The influence of different indenter radius on the force and resistance coefficient values

Figure 4 shows the normal (F_n) and tangential (F_t) forces diagram of $Cu_{50}Zr_{50}$ MGs during the indentation (stage 1), scratching (stage 2) and retraction (stage 3) process with different indenter radius. In the first part of the indentation stage and the last part of the retraction stage, the F_n and F_t values are zero because there is no impact between the indenter and the sample. During the machining process with increasing indenter radius, the amount of material being extruded increases, leading to

the necessary force required to process materials also increased. So, the force value increases as the increasing indenter radius [10]. This phenomenon can be observed in both normal and tangential forces diagram in Figure 4(a) and Figure 4(b), respectively.

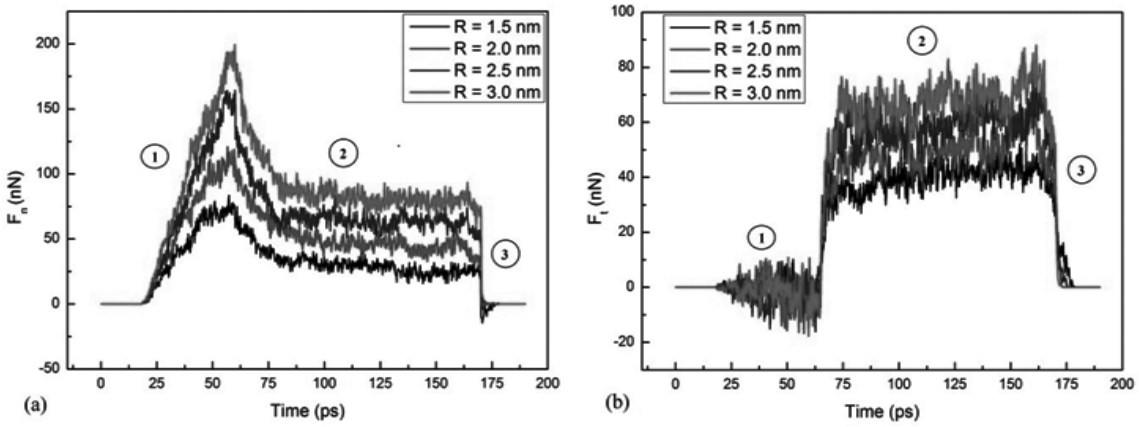

Figure 4. *(a) Normal and (b) tangential force diagram of $Cu_{50}Zr_{50}$ MGs during the indentation, scratching and retraction process with different indenter radius*

During the indentation stage, the normal force F_n rapidly increases to the peak value, while the tangential force F_t fluctuates slightly around the zero. However, after the beginning of the scratching stage, the tangential force F_t rises strongly due to the formation of the chips are started, while the normal force F_n suddenly decreases because of the contact area between the indenter and the sample reduces. This reduction of the contact area is due to the kinematics of the process. A gap is formed between the backside of the indenter and the substrate at the beginning of the scratching stage. Then, a stable phase for both F_n and F_t is observed and maintained until the scratching process ends. However, the strong fluctuations of F_n and F_t appear in this stable phase in all test cases. The reason is due to the vibration generated by the continuous collision between the indenter and the substrate, resulting in the normal force and tangential force also fluctuates. The vibration in the tangential force is stronger than that in the normal force. Finally, both F_n and F_t quickly reduce to zero during the retraction stage. There is no difference between F_n and F_t in all simulations.

The resistance coefficient is determined as the ratio between tangential force and normal force, which is evaluated to depict the mechanical response of $Cu_{50}Zr_{50}$ MGs under the scratching process. The resistance coefficient diagram of $Cu_{50}Zr_{50}$ MGs at different indenter radius under the scratching process is shown in Figure 5. In all four different indenter radius cases, the curves present common features: first, the resistance coefficient increases suddenly at the beginning phase of scratching process, and then vibrates strongly around a constant average value when scratching is stable. It can be observed that the resistance coefficient is larger for smaller indenter radius.

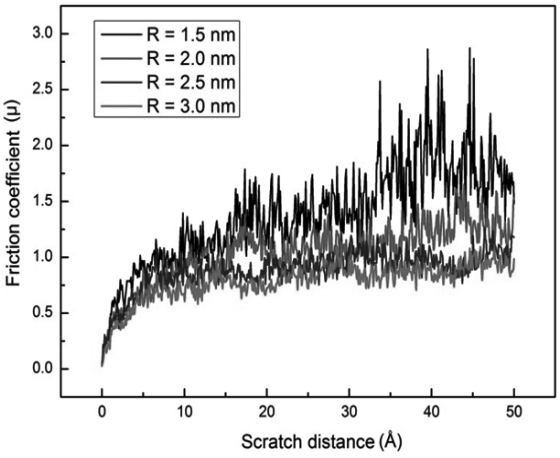

Figure 5. *Resistance coefficient of $Cu_{50}Zr_{50}$ MGs with different indenter radius under the scratching process*

The resistance coefficient values are smaller than 1 for the indenter radius of 2.5 and 3.0 nm, while these values are greater than 1 for the indenter radius of 1.5 and 2.0 nm. Particularly, the resistance is significantly high with the indenter radius of 1.5 nm. The resistance coefficient tends to increase as increasing scratching distance. The changes in the resistance coefficient above can be explained

by the influence of the indenter size. The cutting dominates because most of the indenter volume sinks in the substrate, while the sliding is prioritized in the scratching process. This also confirms that the indenter radius has a significant influence on the mechanism of deformation and mechanical properties of $Cu_{50}Zr_{50}$ MGs during the machining process [9].

4. Conclusion

The mechanical properties and deformation behaviors of $Cu_{50}Zr_{50}$ MGs under indentation and scratching process are investigated by using MD simulations. The conclusions are listed as follows:

(1) The machining zone increases, while the pile-up height decreases as increasing indenter radius.

(2) The hardness values reduce with a bigger radius of indenter and range from 7.94 to 13.33 GPa.

(3) The force increases, however, the resistance coefficient decreases as the indenter radius increases.

Reference

[1]. Wright, W. J., Liu, Y., Gu, X., Van Ness, K. D., Robare, S. L., Liu, X., ... &Dahmen, K. A. Experimental evidence for both progressive and simultaneous shear during quasistatic compression of a bulk metallic glass. *Journal of Applied Physics*, 2016, **119(8)**, 084908.

[2]. Liu, Z. Y., Wang, G., Chan, K. C., Ren, J. L., Huang, Y. J., Bian, X. L., ... &Zhai, Q. J. Temperature dependent dynamics transition of intermittent plastic flow in a metallic glass. I. Experimental investigations. *Journal of Applied Physics*, 2013, **114(3)**, 033520.

[3]. Hilzinger, H. Applications of metallic glasses in the electronics industry. *IEEE Transactions on Magnetics*, 1985, **21(5)**, 2020-2025.

[4]. Bailey, N. P., Schiøtz, J., & Jacobsen, K. W. Simulation of Cu-Mg metallic glass: Thermodynamics and structure. *Physical Review B*, 2004, **69(14)**, 144205.

[5]. Wang, Y., Zhang, J., Wu, K., Liu, G., Kiener, D., & Sun, J. Nanoindentation creep behavior of Cu–Zr metallic glass films. *Materials Research Letters*, 2018, **6(1)**, 22-28

[6]. Bhatia, M. A., Rajagopalan, M., Darling, K. A., Tschopp, M. A., & Solanki, K. N. The role of Ta on twinnability in nanocrystalline Cu–Ta alloys. *Materials Research Letters*, 2017, **5(1)**, 48-54.

[7]. Kazanc, S. Molecular dynamics study of pressure effect on crystallization behaviour of amorphous CuNi alloy during isothermal annealing. *Physics Letters A*, 2007, **365(5-6)**, 473-477.

[8]. Ye, Y., Yang, X., Wang, J., Zhang, X., Zhang, Z., & Sakai, T. Enhanced strength and electrical conductivity of Cu–Zr–B alloy by double deformation–aging process. *Journal of Alloys and Compounds*, 2014, **615**, 249-254.

[9]. Zhu, P. Z., Hu, Y. Z., Wang, H., & Ma, T. B. Study of effect of indenter shape in nanometric scratching process using molecular dynamics. *Materials Science and Engineering: A*, 2011, **528(13-14)**, 4522-4527.

[10]. AlMotasem, A. T., Bergström, J., Gåård, A., Krakhmalev, P., & Holleboom, L. J. Atomistic insights on the wear/friction behavior of nanocrystalline ferrite during nanoscratching as revealed by molecular dynamics. *Tribology letters*, 2017, **65(3)**, 101.

ẢNH HƯỞNG CỦA BÁN KÍNH DỤNG CỤ ĐẾN TÍNH CHẤT CƠ HỌC VÀ HIỆN TƯỢNG BIẾN DẠNG CỦA HỢP KIM VÔ ĐỊNH HÌNH $Cu_{50}Zr_{50}$ TRONG QUÁ TRÌNH TẠO LÕM VÀ CÀO XƯỚC

Tóm tắt:

Trong bài báo này, sự kết hợp giữa quá trình tạo lõm và cáo xước được thực hiện để phân tích cơ chế biến dạng và các tính chất cơ học của hợp kim vô định hình $Cu_{50}Zr_{50}$ sử dụng phương pháp mô phỏng động lực học phân tử. Cơ chế biến dạng và các tính chất cơ học của hợp kim vô định hình $Cu_{50}Zr_{50}$ được đánh giá thông qua hình thái bề mặt, chiều cao vật liệu bị đùn lên, độ cứng, lực và hệ số cản trong quá trình mô

phỏng. Các ảnh hưởng của giá trị bán kính dụng cụ khác nhau được phân tích rất rõ ràng. Kết quả cho thấy rằng vùng biến dạng tăng lên với bán kính dụng cụ lớn hơn. Chiều cao vật liệu bị đùn lên và độ cứng giảm khi bán kính dụng cụ tăng lên. Giá trị độ cứng đạt được trong khoảng từ 7.94 đến 13.33 GPa. Lực tác dụng tăng lên, tuy nhiên, hệ số cản giảm xuống khi bán kính dụng cụ tăng lên.

Từ khóa: *Hợp kim vô định hình $Cu_{50}Zr_{50}$; quá trình tạo lõm; quá trình cào xước; hệ số cản.*